

# Prediction of L-Ascorbic Acid using FTIR-ATR Terahertz Spectroscopy Combined with Interval Partial Least Squares (iPLS) Regression \*

Diding SUHANDY<sup>\*1</sup>, Meinilwita YULIA<sup>\*2</sup>, Yuichi OGAWA<sup>\*2</sup>, Naoshi KONDO<sup>\*2</sup>

## Abstract

In this study iPLS regression was used to select the efficient spectral regions and variables to develop a calibration model for L-ascorbic acid (L-AA) determination using FTIR-ATR terahertz (THz) spectroscopy. The objectives of using iPLS were to improve the prediction performance of L-AA determination and to show mapping of contribution of high and low frequency in determining L-AA. The result obtained by iPLS model with 5 PLS factors was superior than that of full-spectrum PLS model with 10 PLS factors when 7 spectral regions and 70 variables were selected. Prediction performance of L-AA can be improved by using iPLS model with higher ratio prediction to deviation (RPD) value.

[Keywords] L-ascorbic acid, FTIR-ATR THz spectroscopy, iPLS regression, variable selection, calibration model, inter-molecular bonding

## I Introduction

L-ascorbic acid (L-AA), also known as vitamin C, is a water-soluble vitamin. It is found widely in most plant materials, such as fruits and vegetables. In humans, however, L-AA cannot be synthesized because humans have lost the ability to produce L-gulonolactone oxidase, the enzyme necessary for its production (Gershoff, 1994). For this reason, many recently developed food products, such as juices and sport drinks are fortified with vitamin C.

L-AA is an essential nutrient and antioxidant and therefore, it has an important role in health. Hence, there is increasing demand to know the levels of L-AA consumed in both fresh and processed product. However, the concentration of L-AA in fresh food, such as fruits and vegetables, is subject to degradation. It is also subject to degradation during processing like heating, etc. (Lee and Kader, 2000). For this reason, it is highly desired to be able to quantify L-AA concentrations in foods, especially in juice or sports drink, throughout production and the distribution supply chain for quality control purposes.

Several non-spectroscopic methods for L-AA determination have been reported. These conventional methods of L-AA determination include colorimetry, titrimetry, chemiluminescence, fluorometric, chromatographic and electrochemical methods (Arya *et al.*, 2000). Each of these methods though has limitations. For example, although the titrimetry method using dichlorophenolindophenol as the titrant

is rapid, the titrant itself is unstable and must be standardized before use. Chromatographic methods are accurate, but expensive and time consuming. Recently, the use of a FTIR (Fourier transform infrared) spectroscopic based method for L-AA determination has become popular. It is simple, fast and free from chemical waste. With the rapid development of computers and FTIR instrumentation the price of equipment has come down and enhanced capabilities have been established. Today, an FTIR instrument is the standard for organic compound identification work in modern analytical laboratories.

In the previous work, Suhandy *et al.* (2012a) used Fourier transform infrared-attenuated total reflectance terahertz (FTIR-ATR THz ) spectroscopy for L-AA concentration determination in aqueous solution combined with full-spectrum PLS (FS-PLS) regression. However, for practical application it is important to develop a robust calibration model with a high prediction performance. When using a FS-PLS regression, it is possible to include unrelated and unimportant spectrum characteristics in the calibration model that results in over-fitting. If over-fitting occurs, the model will generally have a poor predictive performance. To avoid this problem, it is a very important step to construct a calibration model with only a selected subset of wavenumbers instead of using all the wavenumbers. A robust calibration model with high prediction performance can be developed with properly selected variables that contain only the

\* Partly presented at the IEEE / SICE International Symposium on System Integration SII2011 at Kyoto University, Kyoto, Japan in December 20-22, 2011.

\*1 JSAM Member, Corresponding author, Graduate School of Agriculture, Kyoto University, Sakyo ku, Kyoto 606-8502, Japan; diding2004@yahoo.com

\*2 JSAM Member, Graduate School of Agriculture, Kyoto University, Sakyo ku, Kyoto 606-8502, Japan

important and relevant information to the target variables.

In general, there are two methods for variable selection. The first one is a single variable selection based method. The main objective of this method is to select proper the wavenumber or wavelength to include in the calibration model. In this method, the importance of each variable is directly calculated on the basis of the statistical features of the variables and the calibration model. Uninformative variable elimination by PLS (UVE-PLS) proposed by Centner *et al.* (1996), iterative predictor weighting (IPW) PLS by Forina *et al.* (1999) and competitive adaptive reweighted sampling (CARS) introduced by Li *et al.* (2009) are examples of this kind of variable selection method. UVE-PLS extended along with wavelet transformation was proposed by Shao *et al.* (2004).

The second one is a selection method based on a spectral region instead of using a single variable. It is based on the fact that a region of consecutive wavenumbers or wavelength has to be selected simultaneously, because the spectra have continuous features. In this method, one or more important and relevant spectral region selected for the calibration model that result in a statistically stable and robust calibration model. Interval PLS (iPLS), moving window PLS (MWPLS), genetic algorithm PLS (GA-PLS) are examples of this kind of variable selection method (Nørgaard *et al.*, 2000; Leardi and Nørgaard, 2004; Jiang *et al.*, 2002; Chen *et al.*, 2010). Another example is searching combination MWPLS (SCMWPLS) as an extension of the MWPLS method (Du *et al.*, 2004; Kang *et al.*, 2006; Kasemsumran *et al.*, 2006). In recent work, genetic algorithm-based wavelength selection (GAWLS) was introduced by Arakawa *et al.* (2011).

In this work, the spectral region selection method, based on iPLS, was used to develop a calibration model for L-AA concentration determination in aqueous solution with high prediction performance. Nørgaard *et al.* (2000) first proposed the iPLS method. The objective of iPLS is to split the spectra into some smaller equidistant subintervals, and develop PLS models on each subinterval. Then, the best subintervals are determined on the basis of the root mean squared error of cross-validation (RMSECV) values. The RMSECV is calculated as follows:

$$RMSECV = \sqrt{\frac{\sum_{i=1}^n (\hat{y}_i - y_i)^2}{n}} \quad (1)$$

where  $n$  is the number of samples in the calibration sample set,  $y_i$  is the actual value for sample  $i$  and  $\hat{y}_i$  is the predicted value for sample  $i$  when the model is constructed with sample  $i$  removed (Romia and Bernardes, 2009).

In this study, the FTIR-ATR THz spectroscopy technique

was applied to predict the concentration of L-AA in aqueous solution. When calibrating the PLS model, iPLS regression was used. First, the spectral data was split into equidistant spectral subintervals by iPLS; then subintervals which had lower RMSECV than the average RMSECV were selected. Finally, the iPLS model was developed using these selected subintervals. The prediction performance of the iPLS model was tested with the samples independent from the prediction sample set. The overall results were compared and discussed in comparison with results obtained in the previous report using a full-spectrum PLS (FS-PLS) calibration model (Suhandy *et al.*, 2012a).

## II Materials and Methods

### 1. L-Ascorbic Acid (L-AA)

L-AA powder (L (+) - Ascorbic Acid, Wako Pure Chemical Industries, Ltd., Japan) was used to prepare L-AA solutions by dissolving the powder in distilled water. The solutions were stirred well using a mixer (Tube Mixer TRIO HM-, AS ONE, Japan). In this study, 55 samples of L-AA solution were used as samples. The concentration of L-AA solutions ranged from 0 - 21 % (mass / mass (w/w)).

The samples were divided into two sample sets, a calibration and a cross-validation sample set (35 samples), as well as a prediction sample set (20 samples). Using the calibration and cross-validation sample sets, calibration models were developed using iPLS regression and full cross-validation was conducted on each calibration model developed. Performance of the calibration models finally were evaluated based on measurements of the prediction sample set.

### 2. FTIR-ATR THz device

THz spectra of L-AA solution were acquired using a Fourier-transform infrared (FTIR) based spectrometer (FARIS-1S, JASCO Corp., Japan) (Suhandy *et al.*, 2012a). In this spectrometer, a special light source (high pressure mercury lamp) was used as a THz generating device. This lamp has a low spectral intensity at low frequency (Hangyo *et al.*, 2000). To solve this problem, we used a silicon beam splitter which has a high transmittance in the terahertz region instead of mylar. A sample chamber with an ATR unit was installed on the spectrometer. In this ATR unit, a silicon prism is used as an internal reflection element (IRE). This has a high refractive index in terahertz region. The spectrometer was also equipped with a room-temperature pyroelectric sensor made from deuterated L-alanine triglycine sulfate (DLTGS) as a detector. Software of spectral manager for windows (JASCO Spectral Manager, JASCO Corp., Tokyo, Japan) was used to control the spectral acquisition process.

### 3. FTIR-ATR THz spectral acquisition method

For FTIR-ATR THz measurement, 300  $\mu\text{L}$  of the L-AA solution sample was pipetted quickly onto the silicon prism surface using a micro pipette. The THz spectra of the L-AA solutions were measured in the range 20 - 450  $\text{cm}^{-1}$  with a 16  $\text{cm}^{-1}$  resolution. Each spectrum consisted on average of 200 scanning spectra. The air reference was measured between every 5 samples. The intensity of the sample and reference was obtained in a single beam (SB) unit. During THz spectral measurement, the temperature and the relative humidity in the laboratory were kept around 25  $^{\circ}\text{C}$  and 70 %, respectively. Using Eq. (2), we calculated the absorbance value of the sample.

$$A(\nu) = -\log_{10} \frac{S(\nu)}{R(\nu)} \quad (2)$$

where

$A(\nu)$  is the absorbance at wavenumber  $\nu$  and  
 $S(\nu)$  is the intensity of sample at wavenumber  $\nu$  and  
 $R(\nu)$  is the intensity of air reference at wavenumber  $\nu$ .

The calculated absorbance value was corrected using the ATR correction function provided in the software (JASCO Spectral Manager, JASCO Corp., Tokyo, Japan). The corrected value was used for subsequent analysis.

### 4. Calibration model using interval PLS (iPLS) regression

First, the full spectrum (20 - 400  $\text{cm}^{-1}$ ) was divided into 11 equidistant subintervals. Then the PLS regression was developed for each subinterval. The PLS calibration model was performed with commercial multivariate analysis software; The Unscrambler® version 9.8 (CAMO, Oslo, Norway). For each subinterval, root mean square error of calibration (RMSEC) and the RMSECV value were calculated. For the iPLS calibration model, the calibration and validation was developed on the selected intervals. The average RMSECV of a subinterval was used as threshold value for selection of appropriate subintervals. Only subintervals which had a lower RMSECV than the threshold value were selected for the iPLS regression model. For the prediction data set, the standard error of prediction (SEP) and bias were used instead of RMSEP (root mean standard error of prediction). As mentioned by Agelet and Hurburgh (2010), SEP is corrected for the bias value (or systematic error); thus when reporting SEP, bias must be reported as well. The square root of mean standard error of prediction (RMSEP) is related to SEP and bias according to Eq. (3) (Agelet and Hurburgh., 2010). RMSEP can be reported alone, especially when the bias is small.

$$RMSEP^2 = SEP^2 + bias^2 \quad (3)$$

To evaluate the performance of the prediction, two

dimensionless parameters RPD (ratio prediction to deviation) and RER (ratio error range) values were used. The RPD value is the standard deviation (SD) in reference values of the cross-validation samples divided by the SEP (standard error of prediction). The RER is the range (difference between the maximum and minimum value) in reference values of the cross-validation samples divided by the SEP. When RPD is greater than 3 and RER greater than 10 the calibration model is considered a successful (Williams and Sobering, 1996; Malley *et al.*, 2002; Lorenzo *et al.*, 2009). The equation for RPD and RER are:

$$RPD = \frac{SD}{SEP} \quad (4)$$

$$RER = \frac{(\text{maximum} - \text{minimum})_{\text{reference value}}}{SEP} \quad (5)$$

## III Results and Discussion

### 1. Developing and evaluating calibration models using full spectrum PLS (FS-PLS) regression

Using the full spectrum (20 - 400  $\text{cm}^{-1}$ ), a calibration model was developed using PLS regression based on Savitzky-Golay (SG) first derivative spectra pre-processing. This full spectrum has 110 variables. In this study, the SG first derivative for smoothing used 11 data points and a polynomial order of 2 was used for both FS-PLS and iPLS regression. Using 11 data points for smoothing, the calibration model resulted in the lowest RMSECV value. Fig. 1 shows the calibration and validation results for L-AA determination using FS-PLS regression.

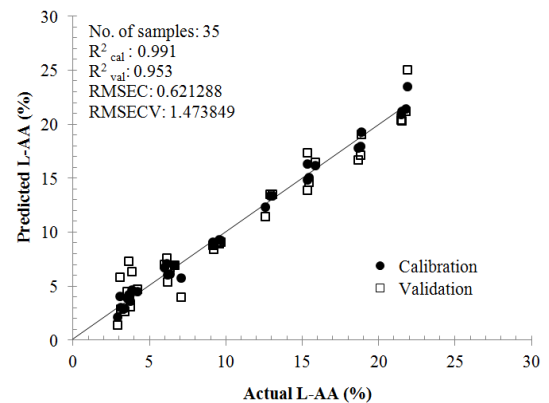


Fig. 1 Calibration and validation result for L-AA determination using FS-PLS regression

### 2. Developing and evaluating calibration models using interval PLS (iPLS) regression

Using iPLS regression, calibration models were developed based on pre-processing of SG first derivative spectra for 11

subintervals. Each subinterval consists of 10 variables. Table 1 shows the calibration and cross-validation results. In general, it is clear that at lower frequencies (less than  $200\text{ cm}^{-1}$ ) the RMSEC and RMSECV values were lower than at higher frequencies, except for the first subinterval. It can be said that the performance of the calibration model at lower frequencies was better than that at higher frequencies.

The high value of RMSEC and RMSECV in the first subinterval may be a result of low light intensity or energy in this subinterval. This low light intensity may be an artifact of the low performance of the Silicon beam splitter during the initiation of the high pressure mercury lamp used in this study. For this reason, this subinterval may lack adequate spectral information, due to a low SNR resulting poor performance of the calibration model in this subinterval.

To elucidate the reason for the poor calibration results at higher frequencies, spectra of the same sample at different temperatures ( $25\text{ }^{\circ}\text{C}$  and  $40\text{ }^{\circ}\text{C}$ ) was acquired using the FTIR-ATR THz spectrometer equipped with a temperature controller. The temperature controller was positioned below the ATR prism to directly control the temperature of the ATR prism within  $\pm 1\text{ }^{\circ}\text{C}$ . The results are presented in Fig. 2. It was clear that at higher frequencies the spectral differences were larger than that at lower frequencies. In present study, the temperature of the samples (all 55 samples) was not directly controlled (no temperature controller used). This sample temperature difference may occur during spectral acquisition and contribute to the poor calibration results at higher frequencies.

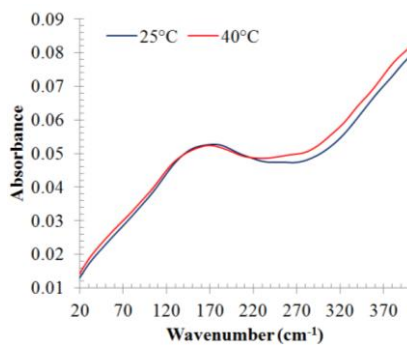


Fig. 2 Typical spectra of L-AA solution in THz region with different temperature

The results presented in Table 1 suggest that the inter-molecular vibration mode detected by THz in the lower frequencies have a significant role in the determination of L-AA concentration. This is consistent with a previous report on glucose concentration determination in aqueous solution using THz spectroscopy (Suhandy *et al.*, 2012b). In aqueous solutions of L-AA, the THz wave spectrum is dominated

strongly by water absorbance. With the presence of L-AA inter-molecular vibration modes develop between water and L-AA and result in weaker water absorbance (See Fig. 3). At higher concentrations of L-AA (L-AA = 21.5 %) the amount of free water is relatively less than at a lower concentration of L-AA (L-AA = 15.3 %). As a result, the absorbance at higher concentrations of L-AA was lower than that at lower concentrations of L-AA. This phenomenon was also found in the previous study using glucose solution (Suhandy *et al.*, 2012b). It can also be said that the spectral differences in Fig. 3 mainly depend on the differences in the volumetric fractions of water in the aqueous solution between the high and low L-AA samples. Taken from this point, it is clear that determination of L-AA concentration in aqueous solution using THz wave is associated with a different mechanism from that of other spectroscopy methods. When using mid and near infrared spectroscopy, determination of L-AA in aqueous solutions is mainly driven by intra-molecular vibration modes arising from specific molecular bonding, such as O-H and C-H bonds.

Table 1 Calibration and cross-validation result using iPLS regression

Subintervals	Wavenumber Range ( $\text{cm}^{-1}$ )	Coefficient of determination ( $R^2_{\text{cal}}$ )	RMSEC (%)	RMSECV (%)
1	19-54	0.365	5.254	6.084
2	58-93	0.835	2.676	3.013
3	96-131	0.799	2.955	3.651
4	135-170	0.630	4.012	4.557
5	174-208	0.736	3.383	3.901
6	212-247	0.610	4.118	4.493
7	251-285	0.461	4.839	5.087
8	289-324	0.566	4.345	5.179
9	328-363	0.209	5.867	6.246
10	366-401	0.209	5.867	7.229
11	405-440	0.068	6.368	6.711

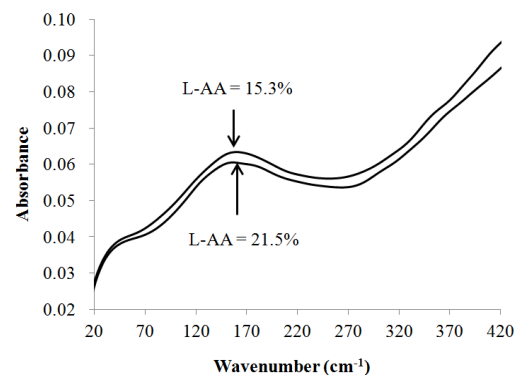


Fig. 3 Typical spectra of L-AA solution in THz region with different concentration

### 3. Intervals selection based on iPLS regression

Based on Table 1, RMSECV was plotted for the 11 subintervals (Fig. 4). RMSECV is mainly used to compare the prediction performance of iPLS and FS-PLS calibration models (Pedersen *et al.*, 2003; Di Anibal *et al.*, 2011). In this study, the average value of RMSECV was used as a threshold for subinterval selection. Subintervals which had a lower RMSECV than the threshold will be selected for development of the iPLS regression model. As seen in Fig. 4, subintervals 2, 3, 4, 5, 6, 7 and 8 have a lower or a similar value of RMSECV to that of the threshold value. For this reason, these subintervals were selected for the iPLS calibration model.

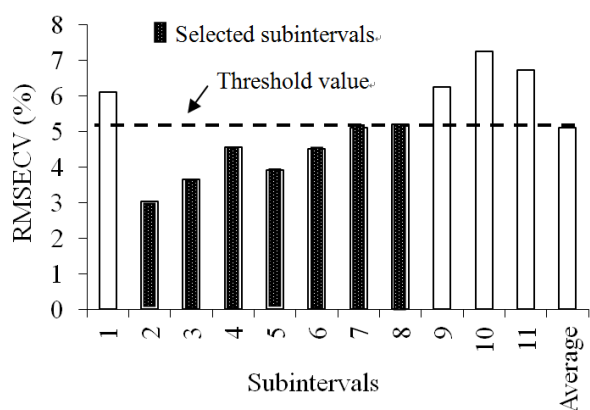


Fig. 4 Subinterval selection using RMSECV calculated from PLS regression in each subinterval

To avoid over-fitting, determining the number of PLS factors to include in the calibration model is a very crucial step. Several studies have reported the use of statistical parameters to evaluate the appropriate number of PLS factors, such as RMSECV and Durbin Watson (DW) values (Gowen *et al.*, 2011). In this study, RMSECV was used for the evaluation of the appropriate number of PLS factors (Chen *et al.*, 2012; Mantanus *et al.*, 2010). Fig. 5 shows a plot between RMSECV and the number of PLS factors for FS-PLS and iPLS. For FS-PLS, the lowest value of RMSECV was obtained with 10 PLS factors. For iPLS, a calibration model using 5 PLS factors had the lowest value of RMSECV. These calibration models were selected as the best FS-PLS and iPLS calibration model respectively, and were used for the prediction of L-AA concentrations.

Fig. 6 shows a scatter plot between actual and predicted L-AA concentrations for both the calibration and validation model using the selected subintervals (subintervals 2, 3, 4, 5, 6, 7 and 8) in the range 58 - 324  $\text{cm}^{-1}$ . The iPLS calibration model (Fig. 6) was not quite as good as the FS-PLS

calibration model (Fig. 1). However, the iPLS calibration model was simpler with only 5 PLS factors compared to the 10 PLS factors in the FS-PLS calibration model. Moreover, the prediction results were used to evaluate the performance of iPLS and FS-PLS calibration model.

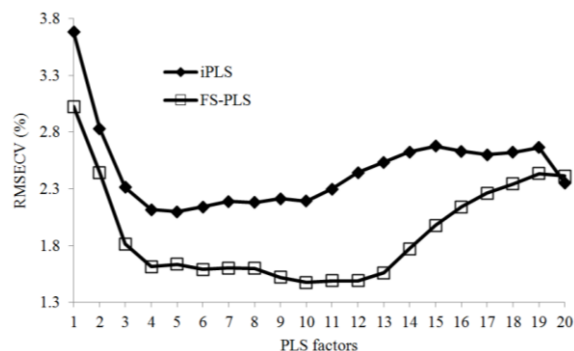
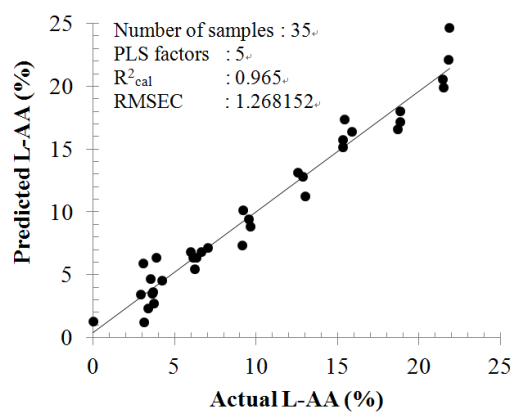
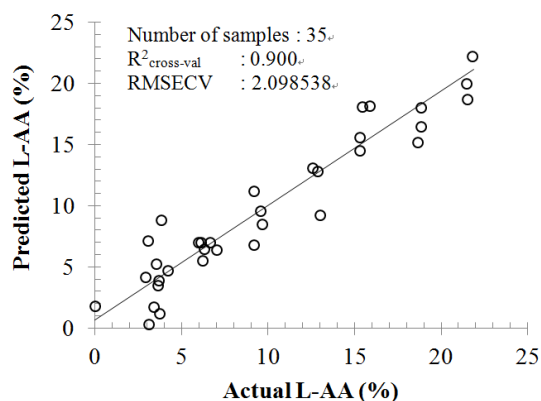


Fig. 5 Number of PLS factors versus RMSECV for the FS-PLS and iPLS calibration model for L-AA prediction



(a) Calibration



(b) validation

Fig. 6 (a) Plot of actual vs. predicted for calibration model for L-AA determination and (b) plot of actual vs. predicted for validation result for L-AA determination using selected subintervals in the range 58 - 324  $\text{cm}^{-1}$  using iPLS

#### 4. Predicting the concentration of L-AA using the FS-PLS and iPLS calibration models

Fig. 7 shows the results for L-AA concentration determination based on the FS-PLS and iPLS calibration models. From the RPD value, it can be seen that the SEPs were much lower than the standard deviation (SD) of reference data for both FS-PLS and iPLS. This indicates that an accurate calibration model for spectroscopy-based determination of L-AA concentration using FTIR-ATR THz spectroscopy can be developed.

The prediction results from the iPLS calibration model were better than those from the FS-PLS regression method. The SEP was 2.146 % for the FS-PLS calibration model. Using the iPLS calibration model the SEP was improved to be 1.490 %. The RPD and RER values of the iPLS calibration model were also better than that of the FS-PLS calibration model. At the same time though, the bias was much higher in the iPLS model. For practical use, this bias must be corrected in order to get reliable prediction results. Further investigation will be needed to clarify the sources of this bias.

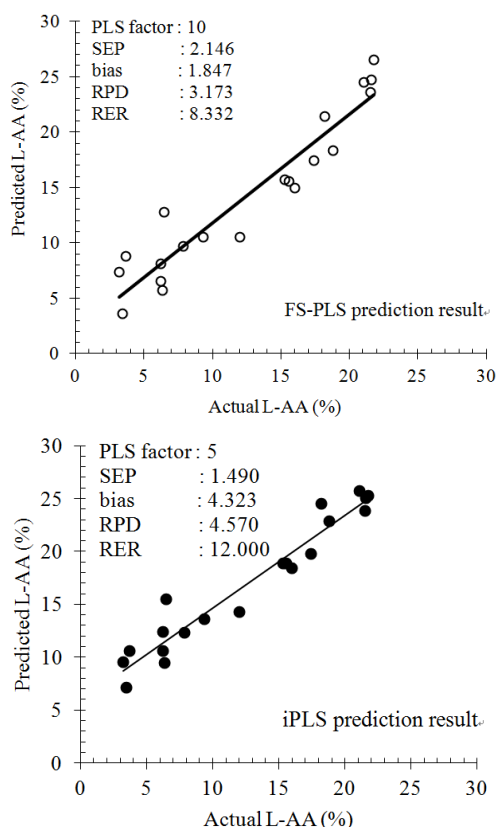


Fig. 7 Scatter plot of actual vs. predicted L-AA calculated using FS-PLS and iPLS calibration model

#### IV Summary and Conclusions

In this study, measurement of L-AA concentrations in aqueous solution were successfully demonstrated using

FTIR-ATR THz spectroscopy combined with an effective wavenumber selection algorithm. The iPLS model for determination of L-AA concentration performed better at lower frequencies than at higher frequencies. This is thought to be due to the influence of inter-molecular vibration modes in lower frequencies, whereas at higher frequencies the intra-molecular vibration mode is influential. Using the iPLS regression with the selected subintervals, the prediction of L-AA concentrations can be optimized; SEP was improved from 2.146 to 1.490 %. The RPD and RER values were also improved. However for practical use, a method for bias correction is needed.

#### Acknowledgements

This work was supported in part by KAKENHI (Grant-in-Aid for challenging Exploratory Research No. 23658209). The authors gratefully acknowledge the financial support provided by that project. The authors also acknowledge to Garry J Piller, professor of G30 of Graduate School of Agriculture Kyoto University for his final proof to this manuscript.

#### References

- Agelet, L. E. and C. R. Hurburgh, Jr. 2010. A tutorial on near infrared spectroscopy and its calibration. *Critical Reviews in Analytical Chemistry* 40:246-260.
- Arakawa, M. Y. Yamashita and K. Funatsu. 2011. Genetic algorithm-based wavelength selection method for spectral calibration. *Journal of Chemometrics* 25:10-19.
- Arya, S. P. M. Mahajan and P. Jain. 2000. Non-spectrophotometric methods for the determination of Vitamin C. *Analytica Chimica Acta* 417:1-14.
- Centner, V. D. L. Massart, O. E. de Noord, S. de Jong, B. M. Vandeginste and C. Sterna. 1996. Elimination of uninformative variables for multivariate calibration. *Analytical Chemistry* 68:3851-3858.
- Chen, Q., P. Jiang and J. Zhao. 2010. Measurement of total flavones content in snow lotus (*Saussurea involucre*) using near infrared spectroscopy combined with interval PLS and genetic algorithm. *Spectrochimica Acta Part A: Molecular and Biomolecular Spectroscopy* 76:50-55.
- Chen, Q., Z. Guo, J. Zhao and Q. Ouyang. 2012. Comparisons of different regressions tools in measurement of antioxidant activity in green tea using near infrared spectroscopy. *Journal of Pharmaceutical and Biomedical Analysis* 60:92-97.
- Di Anibal, C. V., M. P. Callao and I. Ruisanchez. 2011. <sup>1</sup>H NMR variable selection approaches for classification. A case study: The determination of adulterated foodstuffs. *Talanta* 86:316-323.
- Du, Y. P., Y. Z. Liang, J. H. Jiang, R. J. Berry and Y. Ozaki. 2004. Spectral regions selection to improve prediction ability of PLS

- models by changeable size moving window partial least squares and searching combination moving window partial least squares. *Analytica Chimica Acta* 501:183-191.
- Forina, M., C. Casolino and M. C. Pizarro. 1999. Iterative predictor weighting (IPW) PLS: a technique for the elimination of useless predictors in regression problems. *Journal of Chemometrics* 13:165-184.
- Gershoff, S. N. 1994. Vitamin C (ascorbic acid): New roles, new requirements. *Nutrition Review* 52:313-326.
- Gowen, A. A., G. Downey, C. Esquerre and C. P. O'Donnell. 2011. Preventing over-fitting in PLS calibration models of near-infrared (NIR) spectroscopy data using regression coefficients. *Journal of Chemometrics* 25:375-381.
- Hangyo, M., T. Nagashima and S. Nashima. 2000. Spectroscopy by pulsed terahertz radiation. *Measurement Science and Technology* 13:1727-1738.
- Jiang, J. H., R. J. Berry, H. W. Siesler and Y. Ozaki. 2002. Wavelength interval selection in multicomponent spectral analysis by moving window partial least-squares regression with application to mid-infrared and near-infrared spectroscopic data. *Analytical Chemistry* 74: 3555-3565.
- Kang, N., S. Kasemsumran, Y. A. Woo, H. J. Kim and Y. Ozaki. 2006. Optimization of informative spectral regions for the quantification of cholesterol, glucose and urea in control serum solutions using searching combination moving window partial least squares regression method with near infrared spectroscopy. *Chemometrics and Intelligent Laboratory Systems* 82: 90-96.
- Kasemsumran, S., Y. P. Du, K. Maruo and Y. Ozaki. 2006. Improvement of partial least squares models for in vitro and in vivo glucose quantifications by using near-infrared spectroscopy and searching combination moving window partial least squares. *Chemometrics and Intelligent Laboratory Systems* 82: 97-103.
- Leardi, R. and L. Nørgaard. 2004. Sequential application of backward interval partial least squares and genetic algorithms for the selection of relevant spectral regions. *Journal of Chemometrics* 18:486-497.
- Lee, S. K. and A. A. Kader. 2000. Preharvest and postharvest factors influencing vitamin C content of horticultural crops. *Postharvest Biology and Technology* 20:207-220.
- Li, H., Y. Liang, Q. Xu and D. Cao. 2009. Key wavelengths screening using competitive adaptive reweighted sampling method for multivariate calibration. *Analytica Chimica Acta* 648:77-84.
- Lorenzo, C., T. Garde-Cerdán, M. A. Pedroza, G. L. Alonso and M. R. Salinas. 2009. Determination of fermentative volatile compounds in aged red wines by near infrared spectroscopy. *Food Research International* 42:1281-1286.
- Malley, D. F., L. Yesmin and R. G. Eilers. 2002. Rapid analysis of hog manure and manure-amended soils using near infrared spectroscopy. *Soil Science Society of America Journal* 66:1677-1686.
- Mantanus, J., E. Ziémons, P. Lebrun, E. Rozet, R. Klinkenberg, B. Streeel, B. Evrard and Ph. Hubert. 2010. Active content determination of non-coated pharmaceutical pellets by near infrared spectroscopy: Method development, validation and reliability evaluation. *Talanta* 80: 1750-1757.
- Nørgaard, L., S. Saudland, J. Wagner, J. P. Nielsen, L. Munck and S. B. Engelsen. 2000. Interval partial least-squares regression (iPLS): a comparative chemometric study with an example from near-infrared spectroscopy. *Applied Spectroscopy* 54: 413-419.
- Pedersen, D. K., S. Morel, H. J. Andersen and S. B. Engelsen. 2003. Early prediction of water-holding capacity in meat by multivariate vibrational spectroscopy. *Meat Science* 65: 581- 592.
- Romia, M. B. and M. A. Bernardez. 2009. Multivariate calibration for quantitative analysis. In *Infrared Spectroscopy for Food Quality Analysis and Control*, ed. D. W. Sun, ch. 3, 51-82. Academic Press.
- Shao, X., F. Wang, D. Chen and Q. Su. 2004. A method for near-infrared spectral calibration of complex plant samples with wavelet transform and elimination of uninformative variables. *Analytical and Bioanalytical Chemistry* 378:1382-1387.
- Suhandy, D., M. Yulia, Y. Ogawa and N. Kondo. 2012a. L-ascorbic acid prediction in aqueous solution based on FTIR-ATR terahertz spectroscopy. *Engineering in Agriculture, Environment and Food* 5(4): 152-158.
- Suhandy, D., T. Suzuki, Y. Ogawa, N. Kondo, H. Naito, T. Ishihara, Y. Takemoto and W. Liu. 2012b. A Quantitative study for determination of glucose concentration using attenuated total reflectance terahertz (ATR-THz) spectroscopy. *Engineering in Agriculture, Environment and Food* 5(3): 90-95.
- Williams, P. and D. Sobering. 1996. How do we do it: a brief summary of the methods we use in developing near infrared calibrations. In *Near Infrared Spectroscopy: The Future Waves*, ed. A. M. C. Davies and P. Williams, 185-188. Chichester: NIR Publications.

(Received: 23. April. 2012, Accepted: 12. November. 2012)